

Ordering kinetics of stripe patterns

Denis Boyer and Jorge Viñals

*School of Computational Science and Information Technology,
Florida State University, Tallahassee, Florida 32306-4120.*

(November 13, 2018)

We study domain coarsening of two dimensional stripe patterns by numerically solving the Swift-Hohenberg model of Rayleigh-Bénard convection. Near the bifurcation threshold, the evolution of disordered configurations is dominated by grain boundary motion through a background of largely immobile curved stripes. A numerical study of the distribution of local stripe curvatures, of the structure factor of the order parameter, and a finite size scaling analysis of the grain boundary perimeter, suggest that the linear scale of the structure grows as a power law of time $t^{1/z}$, with $z = 3$. We interpret theoretically the exponent $z = 3$ from the law of grain boundary motion.

64.60.Cn, 47.20.Bp, 05.45.-a

Equilibrium layered phases (characterized by a uniform wavevector $\vec{k}_0 \neq 0$) are often found in systems with competing short and long ranged interactions [1]. Related structures, commonly referred to as stripe patterns, also appear in systems driven outside of thermodynamic equilibrium (e.g., Rayleigh-Bénard convection or parametric surface waves near onset [2]). After changing rapidly a control parameter across a transition or bifurcation point, a uniform state become unstable and configurations with locally ordered stripes appear. Given the underlying translational and rotational invariances of the system, spontaneous evolution leads to a macroscopic sample comprising a large number of grains or domains, each relatively uniform, but oriented along an arbitrary direction, as well as to a large density of defects such as grain boundaries, disclinations and dislocations. Understanding how this structure orders with time, and how the motion of interacting defects contributes to the coarsening rate is the main focus of this paper.

Numerical studies of model equations in *two* spatial dimensions [3–7], as well as recent experiments involving thin films of block copolymers [8] support the idea that the time evolution of layered phases after a quench is statistically self-similar (the statistical self-similarity hypothesis asserts that after a possible transient, consecutive configurations of the coarsening structure are geometrically similar in a statistical sense). As a consequence, any linear scale of the structure (e.g., the average size of a domain or grain) is expected to grow as a power law of time $R(t) \sim t^{1/z}$.

Coarsening of layered phases is not yet well understood. On symmetry grounds, layered phases can be classified as smectics [9,4]. Hence, by analogy with coarsening studies of nematics [10] and O(N) vector models with a nonconserved order parameter [11], one would argue that self-similar coarsening is to be expected with $z = 2$. Although, the possibility of a long time cross over to $z = 2$ has in fact been considered [4], numerical evidence has consistently pointed at values of z in the range

$z = 4 - 5$ [4–7]. More importantly, the self-similarity hypothesis itself has been questioned as different linear scales yield different values of z [6,7]. Furthermore, and in contrast with related research on well understood systems that order at $k_0 = 0$ [12,13], the value of z appears to be modified by the presence of thermal noise.

We present here a numerical investigation of domain coarsening for the Swift-Hohenberg model of Rayleigh-Bénard convection [14]. Briefly, we focus on the region close to onset ($\epsilon \rightarrow 0$, where ϵ is the reduced control parameter) and find that coarsening proceeds in a self-similar manner. We analyze several different characteristic length scales, and find that they are asymptotically proportional to each other. We also find that $z \simeq 3$, independent of thermal noise. We interpret this value of z from the law of grain boundary motion given in [15]. Further from onset ($\epsilon \simeq 0.25$), we recover the results of previous studies, which we interpret as arising from non-adiabatic effects that lead to defect pinning. This fact accounts for both the slower growth seen previously, and its dependence on fluctuations.

The Swift-Hohenberg model of convection in dimensionless units is [14],

$$\frac{\partial \psi}{\partial t} = \epsilon \psi - \frac{\xi_0^2}{4k_0^2} (k_0^2 + \nabla^2)^2 \psi - \psi^3, \quad (1)$$

where ψ is an order parameter related to the vertical fluid velocity at the mid plane of a Rayleigh-Bénard convection cell, ϵ is the reduced Rayleigh number, k_0 is the roll wavenumber, and ξ_0 is a constant that depends on the boundary conditions at the top and bottom plates. For our purposes, we note that $\xi_0 \propto 1/k_0$. The same model has been used to analyze coarsening of lamellar phases in a diblock copolymer [7], and is otherwise believed to be a generic model of the kinetics of stripe formation. There, ψ is the concentration difference between the two monomers [16,17]. For $0 < \epsilon \ll 1$, the stationary solution of Eq. (1) is well approximated by a sinusoidal function of wavenumber k_0 . The transient evolution and domain coarsening is investigated by numerically integrating Eq.

(1) from random initial conditions. All calculations are performed very close to onset ($\epsilon = 0.04$). Details of the numerical algorithm can be found in ref. [15].

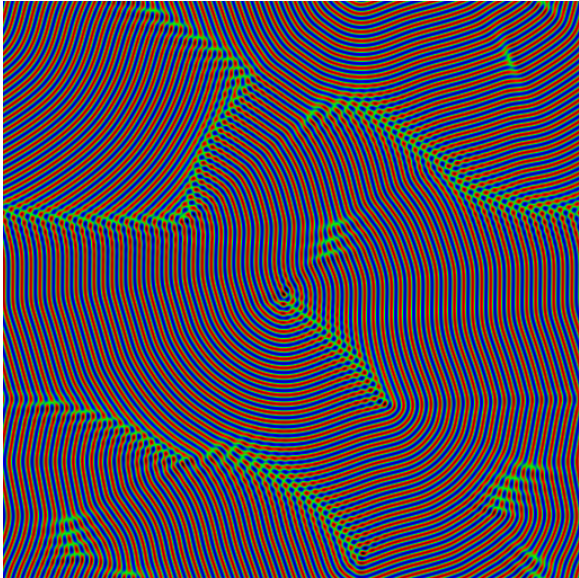


FIG. 1. Order parameter ψ shown in grey scale at time $t = 15000$. Eq. (1) is discretized on a square grid of mesh size $\Delta x = 1$ with 512^2 nodes. The wavelength $\lambda_0 = 2\pi/k_0 = 8\Delta x$. The reduced Rayleigh number is $\epsilon = 0.04$. The initial condition has $\langle \psi \rangle = 0$ and $\langle \psi^2 \rangle = 0.04$.

Figure 1 shows a typical transient configuration. The configuration contains a large amount of grain boundaries that separate domains of different orientation, as well as defects (such as $+1/2$ disclinations and dislocations).

We first present our numerical results for several measures of the linear scale of the structure, including the distribution of stripe curvatures, the order parameter structure factor, and the grain boundary perimeter. Following initial transients, the stripe curvature $\kappa = |\nabla \cdot \vec{n}|$ is a slowly varying field, where \vec{n} denotes the unitary vector normal to the lines of constant ψ . We compute the probability distribution function of stripe curvatures $P(\kappa, t)$ by considering only the subset of points where stripe orientation can be properly defined, *i.e.* the points that are not in the immediate vicinity of any grain boundary nor other defects. Far enough from a defect, $\psi(\vec{r}) = A(\vec{r}) \cos(\vec{k}(\vec{r}) \cdot \vec{r} + \phi)$, with A a slowly varying amplitude. By defining $\zeta(\vec{r}) = \psi^2 + (\vec{\nabla} \psi)^2 / k_0^2$, one has $\zeta(\vec{r}) \simeq A^2$. Note that for stationary parallel stripes of wavenumber k_0 , $\zeta(\vec{r}) = \zeta_0 = 4\epsilon/3$ [2]. We now define defect free regions as those that satisfy $r_m < \zeta/\zeta_0 < r_M$, with $r_m = 0.95$, $r_M = 1.05$ (filter *a*) or $r_m = 0.97$, $r_M = 1.10$ (filter *b*). We have numerically verified that the values of ζ corresponding to a set of moderately curved stripes along their transverse direction remain completely within the intervals defined by both filters *a* and *b*. By contrast, most values of ζ in the vicinity of

a grain boundary are lower than 0.90.

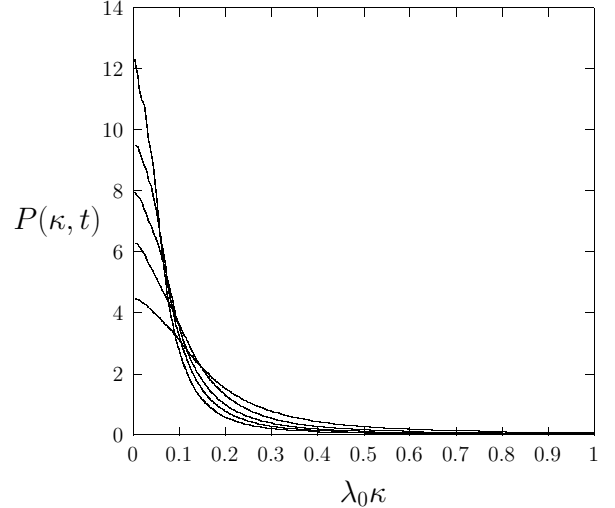


FIG. 2. Probability distribution function of curvatures $P(\kappa, t)$ averaged over 35 independent initial conditions for times ranging from $t = 960$ to $1.6 \cdot 10^4$.

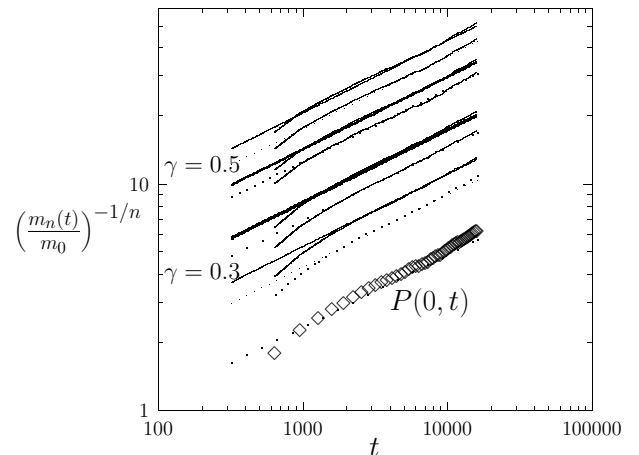


FIG. 3. Moments $m_n(t)$ of $P(\kappa, t)$ obtained with filter *a*. The values of n shown are $1/2, 1, 2, 3$, from top to bottom. The straight lines have a slope of 0.32.

Figure 2 shows $P(\kappa, t)$ at different times, after averaging over 35 independent initial conditions on a square grid of size 1024×1024 (16 grid nodes per wavelength λ_0), at $\epsilon = 0.04$ and using filter *a*. To check for self-similarity we study whether $P(\kappa, t) = t^{1/z} p(\kappa t^{1/z})$. In order to do this, we compute its moments $m_n(t) = \int_0^{\kappa_c(t)} d\kappa \kappa^n P(\kappa, t)$ with $\kappa_c(t)$ defined as $\int_0^{\kappa_c(t)} d\kappa P(\kappa, t) = \gamma \kappa_c(t) P(0, t)$, and γ an arbitrary constant, $0 < \gamma < 1$. We find that $(m_n/m_0)^{-1/n} \propto t^{1/z}$, with the value of z independent of n and γ , thus lending support to the self-similarity hypothesis. Figure 3 shows the results for a few values of n and two values of γ . In addition, the best fit to the

curves yields $1/z \simeq 0.32$ with filter a , and $1/z \simeq 0.34$ with filter b (not shown).

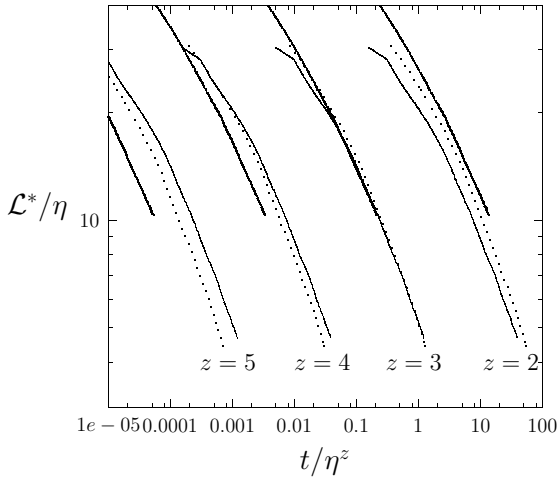


FIG. 4. Finite size scaling analysis of the total grain boundary length, with systems of aspect ratio $\eta = 32, 42.66$ and 64 .

We next present a finite size scaling analysis to independently determine the value of z [18]. Let N_d be the number of grid points for which $\zeta > r_M$ or $\zeta < r_m$. The probability of a point belonging to a defect is $p_d = N_d \Delta x^2 / L^2$, with L the system linear extent. We define a dimensionless defect (*i.e.* grain boundary) perimeter as $\mathcal{L}^* = \eta^2 p_d$, where $\eta = L/\lambda_0$ is the aspect ratio. For short times finite size effects are expected to be negligible, and $p_d \sim t^{-1/z}$. We now introduce a finite size scaling ansatz, valid for any time t ,

$$\mathcal{L}^*(\eta, t) = \eta g(t/\eta^z), \quad (2)$$

with $g(x) \sim x^{-1/z}$ for $x \ll 1$. At fixed $\epsilon = 0.04$, we have numerically computed $\mathcal{L}^*(t)$ with the help of filter a for different aspect ratios: $\eta = 32, 42.66$ and 64 (*i.e.* $\eta = 258/8, 256/6$ and $512/8$; $\Delta x = 1$ in all cases). We have averaged the results over 500, 300 and 100 independent initial conditions respectively. Figure 4 shows our results for the universal curve $g(x)$. The value $z = 3$ leads to curves \mathcal{L}^*/η as a function of t/η^z do not depend on η .

We have also analyzed the Fourier transform of the two-point correlation function of the order parameter, $S(k, t) = \langle \tilde{\psi}_{\vec{k}} \tilde{\psi}_{-\vec{k}} \rangle$, averaged over all possible orientations of \vec{k} and 50 independent initial conditions. Such study is standard [4–6]. If $|k - k_0| \ll k_0$ and $k_0 L(t) \gg 1$, $S(k, t)$ satisfies the scaling form $S(k, t) = k_0^{1-d} L(t) f[(k^2 - k_0^2)L(t)\lambda_0]$, where d the spatial dimension. Analysis of the moments of $S(k, t)$ shows that $L(t) \sim t^{1/z}$ with $1/z \simeq 0.31$. We also find that $S(k_0, t) \sim t^{0.32}$.

Finally, we have verified that the value of the exponent z calculated from either the grain boundary perimeter or the structure factor is not modified by the introduction of random fluctuations into Eq. (1).

The results presented are qualitatively modified further from onset. For example, at $\epsilon = 0.25$ we find that different linear scales of the structure are no longer proportional to each other, and we obtain effective exponents that are in agreement with the values of z reported in earlier studies at $\epsilon \simeq 0.25$ [3,5,6]. We find $1/z \simeq 0.21$ from an analysis of the moments of $S(k, t)$, $1/z \simeq 0.26$ from the grain boundary perimeter, while the moments of the distribution of curvatures yield $1/z \simeq 0.32$.

We next discuss a possible growth mechanism leading to an exponent of $z = 3$, as well as our interpretation for the slower growth that is found when ϵ is not sufficiently small, and its dependence on random fluctuations. Coarsening exponents can be often inferred from the law of motion of the class of defects that control coarsening [19]. A typical transient configuration (Fig. 1) contains a large amount of grain boundaries, as well as other defects such as $+1/2$ disclinations. Grain boundaries move over large distances, whereas disclinations remain largely immobile. Disclinations produce a background of curved rolls that cannot freely relax due to topological constraints (this is in contrast with other coarsening mechanisms discussed in [3,7].) However, at any given point roll relaxation as well as disclination annihilation do occur after the passage of a grain boundary. In ref. [15] we studied the motion of a grain boundary separating two semi-infinite domains of mutually perpendicular rolls, straight on one side, curved on the other. At lowest order in ϵ , those parallel to the boundary are distorted whereas those that are perpendicular to it remain straight. The energy of the configuration decreases by a net displacement of the grain boundary, the effect of which is to replace curved rolls by straight ones of lower energy. Therefore the size of the domain with curved rolls decreases. We showed that if the curvature of the rolls ahead of the boundary is κ , the boundary advances at a speed,

$$v_{gb} \sim \epsilon^{-1/2} \kappa^2. \quad (3)$$

It was shown in [15] that Eq. (3) is in quantitative agreement with a direct numerical solution of Eq. (1) with an initial condition that involves a 90° grain boundary. As seen in Fig. 1, disclinations produce roughly axisymmetric patterns, with a characteristic roll curvature that is inversely proportional to the distance among disclinations. If this distance is proportional to the characteristic linear scale $R(t)$, then dimensional analysis of Eq. (3) suggests $R(t) \sim t^{1/3}$.

These considerations are modified further from onset. The law of grain boundary motion, Eq. (3), is valid only to first order in ϵ . At moderate values of ϵ , the separation of length scales assumed in the derivation of Eq. (3) breaks down (the grain boundary thickness is of order $\lambda_0/\sqrt{\epsilon}$), leading to non-adiabatic effects. Within the amplitude equation formalism, and following the approach

of ref. [20], we have obtained the leading order nonadiabatic corrections, and find that the position of the grain boundary and the phase of the rolls located ahead of it no longer decouple. Equation (3) can be generalized to,

$$v_{gb} = \frac{\epsilon}{3k_0^2 D(\epsilon)} \kappa^2 - \frac{p(\epsilon)}{D(\epsilon)} \cos(2k_0 x_{gb} + \phi), \quad (4)$$

where x_{bg} is the average location of the grain boundary, ϕ is a constant phase and,

$$D(\epsilon) = \int_{-\infty}^{\infty} dx [(\partial_x A_0)^2 + (\partial_x B_0)^2], \quad (5)$$

$$p(\epsilon) = \max_{\theta} \left\{ \frac{3}{4} \int_{-\infty}^{\infty} dx A_0^3(x) \partial_x A_0(x) \cos(2k_0 x + \theta) + \frac{3}{2} \int_{-\infty}^{\infty} dx [2A_0 B_0^2 \partial_x A_0 + A_0^2 B_0 \partial_x B_0] \cos(2k_0 x + \theta) \right\}. \quad (6)$$

The functions $A_0(x)$ and $B_0(x)$ are the amplitudes of the two sets of rolls separating a planar boundary [21], the coefficient $D(\epsilon)$ represents a friction term, and $p(\epsilon)$ the amplitude of a periodic pinning potential. The contribution from non adiabatic effects is typically of the order of,

$$p(\epsilon) \sim \epsilon^2 e^{-|\alpha|/\sqrt{\epsilon}}, \quad (7)$$

where $|\alpha|$ is a constant of order unity. Hence, p behaves non analytically as $\epsilon \rightarrow 0$, but increases extremely fast with ϵ at low values of ϵ . From Eq. (4) we see that at any finite $\epsilon > 0$, there exists a critical curvature κ_g below which $v_{gb} = 0$. Remarkably, pinning becomes noticeable even at $\epsilon = 0.1$ [15], and grain boundaries were seen to advance only by half-integer multiples of the roll wavelength. Therefore we expect that grain boundaries in a coarsening configuration will become pinned over time. We believe that this pinning is the reason behind the lower effective exponents found in previous studies at $\epsilon = 0.25$ [3,6,7], as well as for the related result that random fluctuations added to Eq. (1) consistently lead to larger coarsening rates.

In summary, we have presented results for several independent measures of the linear scale of stripe patterns ordering very near onset, and obtained a coarsening exponent that is very close to $z = 3$. This value can be explained through dimensional analysis of the velocity of a single grain boundary advancing into a background of curved stripes in the limit $\epsilon \rightarrow 0$. This mechanism also predicts increasing corrections to scaling further from onset due to defect pinning.

This research has been supported by the U.S. Department of Energy, contract No. DE-FG05-95ER14566.

- [1] M. Seul and D. Andelman, *Science* **267**, 476 (1995).
- [2] M. Cross and P. Hohenberg, *Rev. Mod. Phys.* **65**, 851 (1993).
- [3] K. Elder, J. Viñals, and M. Grant, *Phys. Rev. Lett.* **68**, 3024 (1992).
- [4] K. Elder, J. Viñals, and M. Grant, *Phys. Rev. A* **46**, 7618 (1992).
- [5] M. Cross and D. Meiron, *Phys. Rev. Lett.* **75**, 2152 (1995).
- [6] Q. Hou, S. Sasa, and N. Goldenfeld, *Physica A* **239**, 219 (1997).
- [7] J. Christensen and A. Bray, *Phys. Rev. E* **58**, 5364 (1998).
- [8] C. Harrison *et al.*, *Science* **290**, 1558 (2000).
- [9] J. Toner and D. Nelson, *Phys. Rev. B* **23**, 316 (1981).
- [10] M. Zapotocky, P. Goldbart, and N. Goldenfeld, *Phys. Rev. E* **51**, 1216 (1995).
- [11] G. Mazenko, in *Formation and interaction of topological defects*, edited by A.-C. Davis and R. Brandenberger (Plenum, New York, 1995).
- [12] J. Gunton, M. San Miguel, and P. Sahní, in *Kinetics of first order phase transitions*, Vol. 8 of *Phase Transitions and Critical Phenomena*, edited by C. Domb and J. Lebowitz (Academic, London, 1983).
- [13] A. Bray, *Adv. Phys.* **43**, 357 (1994).
- [14] J. Swift and P. Hohenberg, *Phys. Rev. A* **15**, 319 (1977).
- [15] D. Boyer and J. Viñals, *Phys. Rev. E* **63**, 061704 (2001).
- [16] Y. Shiwa, *Physics Letters A* **228**, 279 (1997).
- [17] P. Hohenberg and J. Swift, *Phys. Rev. E* **52**, 1828 (1995).
- [18] J. Viñals and D. Jasnow, *Phys. Rev. B* **37**, 9582 (1988).
- [19] A. Bray, *Phys. Rev. E* **58**, 1508 (1998).
- [20] D. Bensimon, B. Shraiman, and V. Croquette, *Phys. Rev. A* **38**, 5641 (1988).
- [21] P. Manneville and Y. Pomeau, *Phil. Mag. A* **48**, 607 (1983).